Korean J. Chem. Eng., 33(7), 2114-2126 (2016)
DOI: 10.1007/s11814-016-0071-0

pISSN: 0256-1115
eISSN: 1975-7220

Adsorptive removal of nickel(II) ions from aqueous environments using gum based and clay based polyaniline/chitosan nanobiocomposite beads and microspheres: Equilibrium, kinetic, thermodynamics and ex-situ studies

Lina Rose Varghese, Devlina Das, and Nilanjana Das†

School of Bio Sciences and Technology, Environmental Biotechnology Division, VIT University, Vellore-632014, Tamil Nadu, India
(*Received 30 November 2015 • accepted 4 March 2016*)

Abstract−The present study was carried out using gum (Ga) based and clay (MMT) based nanobiocomposite beads and microspheres composed of polyaniline NPs (PANI) and chitosan (Ch) as adsorbent for the removal of Ni(II) ions from aqueous environments. Under optimized conditions maximum Ni(II) removal 98.12% was exhibited by clay based nanobiocomposite (PANI-Ch-MMT) beads followed by gum based nanobiocomposite (PANI-Ch-Ga) beads (95.02%), PANI-Ch-MMT microspheres (85.12%) and PANI-Ch-Ga microspheres (75.23%). Equilibrium studies suggested a homogeneous mode of Ni(II) adsorption. Better applicability of pseudo-first order kinetic model suggested physisorption as the underlying phenomenon. Thermodynamic studies showed that adsorption was endothermic and spontaneous. The mechanism of adsorption by PANI-Ch-MMT and PANI-Ch-Ga beads was elucidated using SEM, EDX and FT-IR analyses. *Ex-situ* studies showed a maximum Ni(II) removal of 80.55% from mining wastewater using PANI-Ch-MMT beads in column mode. Regeneration studies suggested that PANI-Ch-MMT beads could be consistently reused up to five cycles.

Keywords: Adsorption, Chitosan (Ch), Polyaniline NPs (PANI), Nickel(II), Wastewater

INTRODUCTION

Environmental pollution has been created from enormous industrial activities, resulting in a massive release of harmful pollutants into the environment [1]. Heavy metals among these pollutants are particularly harmful due to their toxic, carcinogenic and non-biodegradable nature. Among the heavy metals, nickel is of special interest because of its widespread presence in industrial applications [2]. It is present in wastewaters released from industries such as plastic manufacturing, metal finishing, mining, smelting, porcelain enamelling, galvanization, electroplating and nickel-cadmium batteries manufacturing [3]. According to WHO guidelines, the maximum permissible limit of nickel in industrial effluent is 4.1 mg/L and less than 0.1 mg/L in drinking water [4]. Exposure to high concentration of nickel enhances the risk of cancer, thereby affecting lungs, nose and bones. Nickel poisoning causes headaches, dermatitis, dizziness, nausea, vomiting, respiratory distress, cyanosis and extreme weakness [5,6]. In view of toxic effects of nickel on human and animal life, it is necessary to treat nickel-containing industrial effluents before being discharged into the receiving water bodies. The main techniques utilized for the treatment of nickel(II) bearing wastewaters include precipitation, coagulation, evaporation, ion exchange, membrane processing, adsorption and solvent extraction [7]. Among the various remediation techniques, adsorption offers an attractive and cost-effective remediation option and has significant benefits [8]. Effective adsorbents and simple technologies are still in great demand to remove heavy metal ions from aqueous environments.

Nanobiocomposites, which incorporate the advantageous properties of both biopolymers and nanoparticles, have recently received increasing attention as a potential adsorbent in reducing environmental pollution, owing to their high surface area and a wide range of functional groups that they offer for the adsorption process to occur efficiently [9]. The physico-chemical properties of biopolymers are also deterministic in their quality as sorbents, and the presence of a greater number of reactive groups on their chains and high reactivity adds to their adsorption capacity [10]. Nanoparticles are considered as one of the important building blocks in fabrication of nanomaterials because of their basic properties, high surface area to volume ratio. Extremely small size of nanoparticle provides better kinetics for an enhanced rate of metal ion adsorption from aqueous environments. Chitosan, the deacetylated product of chitin extracted from various plants and animals has been reported as a potential biopolymer for the removal of metal ions from aqueous solution due to the presence of amino and hydroxyl groups [11]. Gum Arabic is a complex arabinogalactan that contains a small proportion of proteinaceous materials and has been used in the removal of metal ions [12]. MMT, a clay mineral, has attracted much attention in recent years for the removal of pollutants due to its high adsorption capacity, ion exchange and expansion properties as well as layered structure, high surface area low cost and abundance [13,14]. Polyaniline (PANI) is considered as one of the promising polymers because of its well-defined electrochemical properties, low cost, easy polymerization, high environmental stability and variety

†To whom correspondence should be addressed.
E-mail: nilanjana00@lycos.com

of nanostructured morphologies [15]. Recently, some researches have been directed towards the application of polyaniline and its composites for environmental applications based on the chelating properties of electron donating groups such as amine and secondary amino groups present on the polyaniline polymers [16].

To the best of our knowledge, no report is available so far on the application of gum based and clay based PANI-Ch nanobiocomposites for the effective removal of Ni(II) ions from aqueous environment. Therefore, the present work is focused on the application of gum based nanobiocomposite (PANI-Ch-Ga) and clay based nanobiocomposite (PANI-Ch-MMT) in the form of beads and microspheres for Ni(II) removal from aqueous solution. The process was optimized and adsorption isotherms and kinetics models were studied to describe the experimental data. The adsorption mechanism of Ni(II) onto the beads was further elucidated using SEM, EDX and FT-IR analyses. For practical applications, *ex-situ* studies were also performed to remove Ni(II) from mining wastewater in column mode.

EXPERIMENTAL

1. Materials

All the chemicals used in the present study including cetyltrimethylammonium bromide (CTAB), aniline, ammonium persulfate (APS), chitosan, gum Arabic, montmorillonite (MMT), $Ni(NO_3)_2 \cdot 6H_2O$, NaOH, HCl, paraffin oil, Tween-80, glutaraldehyde and ethanol were of analytical grade and purchased from Sigma Aldrich, India.

2. Synthesis of Polyaniline Nanoparticles

Polyaniline nanoparticles were synthesized following a previously described procedure [17] using CTAB as a surfactant. 1 mL of aniline was added dropwise to 40 ml of the solution containing CTAB (0.5 M). To the above solution 22 g of 1.5 M HCl and 1.23 g of APS were added. The mixture was then kept under vigorous stirring for 3 h at 3 °C for chemical oxidation polymerization to take place. After polymerization reaction, the product was washed with distilled water and ethanol to remove surfactants. The polyaniline nanoparticles were retrieved and dried at 40 °C in hot air oven.

3. Preparation and Characterization of Nanobiocomposite Beads and Microspheres

Gum based nanobiocomposite (PANI-Ch-Ga) beads were prepared following a standard procedure with minor modifications [18]. To a working solution of 100 mL (containing 2% glacial acetic acid), 3% of gum Arabic (Ga) was added and magnetically stirred for 10 min. To this suspension, 0.12% of the previously prepared PANI nanoparticles was dispensed and magnetically stirred for 2 h. Finally, 3% of chitosan was slowly added to the suspension under magnetic stirring condition and the reaction was carried out for 1 h. Beads were formed in 8% NaOH solution after which they were extensively washed with ethanol and distilled water to remove any unreacted fraction and dried in a hot air oven at 60 °C overnight.

PANI-Ch-Ga microspheres were prepared according to the procedure reported in the literature [19] with modifications. 3% of gum Arabic (Ga) was dissolved in 100 mL of 2% acetic acid solution. Once dissolved, 0.12% of PANI nanoparticles was added and sonicated for 30 min and then 3% chitosan was added and magnetically stirred for 2 h. This solution was added dropwise into the dispersion medium which was composed of 100 mL of paraffin oil containing Tween-80 and was stirred for 1 h at room temperature. After 10 min, 1 mL of glutaraldehyde was added to the dispersion medium. Similarly, after 1 h another 1 mL of glutaraldehyde was added to the medium which was then stirred for further 2 h. At the end of this period, gum based nanobiocomposite (PANI-Ch-Ga) microspheres were collected and rinsed with ethanol and distilled water for three times. The microspheres were then dried in a hot air oven at 60 °C for 24 h.

Clay based nanobiocomposite (PANI-Ch-MMT) beads and microspheres were prepared following the same procedure as described above for the preparation of PANI-Ch-Ga beads and microspheres. In both the cases, gum Arabic (Ga) was replaced by montmorillonite (MMT).

The BET surface area of the nanobiocomposite beads and microspheres was calculated following the standard procedure [20]. Thermogravimetric analysis (TGA) was carried out under high purity helium supplied at a purge gas flow rate of 0-1,000 ml min^{-1} (Diamond TG/DTA, Perkin Elmer, USA) in the temperature range of 20-650 °C at a heating rate of 20 °C min^{-1}. The surfaces of the nanobiocomposites were also analyzed using X-ray diffraction analysis (D8 Advance: Bruker, Germany).

4. Batch Adsorption Studies

In the adsorption experiments, the effect of parameters--pH (2.0-12.0), contact time (2-36 h), temperature (10-50 °C), initial Ni(II) concentration (100-1,200 mg L^{-1}) and adsorbent dosage (1.0-6.0 g L^{-1}) on the removal efficiency of Ni(II)--were studied. The experiments were optimized at the desired pH, metal concentration, adsorbent dosage, temperature and contact time using 100 mL of Ni(II) test solution in 250 mL Erlenmeyer flask which were placed in a shaker at required agitation time 120 rpm. At the end of agitation time, the samples were withdrawn and subjected to centrifugation at 8,000 rpm for 5 min. The residual concentration of Ni(II) present in the supernatant was analysed using an atomic adsorption spectrophotometer (AAS). The adsorption capacity (q_e) and the removal percentage (R%) of Ni(II) were calculated according to the following equations:

$$q_e = \frac{C_0 - C_e}{M} \times V \quad (1)$$

$$R(\%) = \frac{C_0 - C_e}{C_0} \times 100 \quad (2)$$

where q_e (mg g^{-1}) is the uptake of metal ion on the adsorbent, C_0 and C_e are the initial and equilibrium concentration of metal ions in the residual solution (mg L^{-1}), V is the volume (L) of metal ion solution used and M is the mass (g) of the adsorbent used.

5. Equilibrium, Kinetic and Thermodynamic Studies

Two parameter isotherms--Langmuir [21], Freundlich [22] and Dubinin-Radushkevich (D-R) [23]--were used to analyze the equilibrium data. The model significance was tested by their correlation coefficients and average percentage error values. For modelling the kinetics of Ni(II) adsorption and to understand the mode and rate of adsorption process, various kinetic models--pseudo-first order

[24], pseudo-second order [25], intraparticle diffusion model and Boyd plot [26]--were used. Thermodynamic studies were conducted by estimating the uptake values at a temperature range of 10-50 °C. The Gibbs free energy, enthalpy and entropy, (ΔG, ΔH, ΔS) are important thermodynamic parameters with respect to the heat requirements and randomness of the process and were obtained using the standard equations [27].

6. Instrumental Analysis

Fourier transformed infrared spectra were recorded on an Avatar 330 model (Thermo Nicolet Co., USA) FT-IR spectrometer. The surface morphology of the nanobiocomposite beads before and after adsorption of Ni(II) ions was analyzed using scanning electron microscopy (SEM) (Stereo Scan LEO, Model-400). EDX analysis were conducted using Noran System Six model Energy Dispersive X-Ray Microanalysis System (Thermo Electron Corporation, Japan) attached to SEM. Accelerating voltage was kept constant at 15 kV, to facilitate the emission of secondary X-rays. Each experiment was repeated at least three times.

7. Effect of Co-ions

Ni(II) adsorption was studied in the presence of co-ions: Cu(II) and Zn(II) in a 2-metal (binary) system and 3-metal (ternary) system. The uptake values of Ni(II) in the presence of co-ions using PANI-Ch-Ga and PANI-Ch-MMT beads were calculated and the experiments were performed in duplicate. Extended Langmuir and Sheindorf Rebhun Shentuck (SRS) models were used to calculate interaction and selectivity factors following the standard equations [28].

8. *Ex-situ* Studies

For *ex-situ* studies, the effluent was collected from mining wastewater on the outskirts of Chennai, Tamil Nadu, India. The concentration of Ni(II) in the effluent was analyzed by using AAS and pH was adjusted to 6.0. A glass column having an internal diameter of 3.0 cm and 15.0 cm in length was employed in the column experiments and packed with the PANI-Ch-MMT beads. The column efficiency was studied at various bed depths (4, 8 and 12 cm), flow rates (1, 3 and 5 mL min^{-1}) and dilutions (0%, 25% and 50%). The area under the breakthrough curves was measured to calculate the total metal adsorbed. The total metal sent to the column and the metal removal percentage was calculated using the standard formula [29].

9. Regeneration Studies

In the regeneration experiments, PANI-Ch-MMT beads were exposed to 0.1 M HNO_3 at a flow rate of 1 mL min^{-1}. After every cycle of adsorption/desorption, the column was washed with deionized water until a pH of 7.0 was attained. The regenerated bed was used in the next sorption cycle. The experiments were performed till the efficiency of the column showed a drastic decrease.

RESULTS AND DISCUSSION

1. Characterization of the Nanobiocomposite Beads and Microspheres

The BET surface area of PANI-Ch-MMT beads and microspheres was found to be 54.23 $m^2 g^{-1}$ and 43.34 $m^2 g^{-1}$, respectively, and in case of PANI-Ch-Ga, the surface area was found to be 46.95 $m^2 g^{-1}$ and 35.48 $m^2 g^{-1}$ for beads and microspheres, respectively.

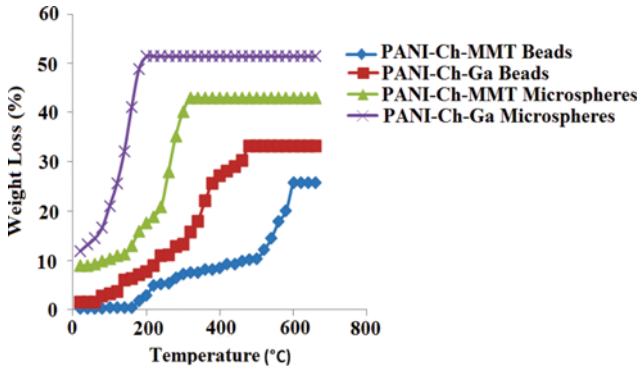

Fig. 1. Thermogravimetric analysis at a temperature range of 20 °C to 660 °C.

Thermogravimetric analysis (TGA) plays an important role in determining the thermal stability of the composite. Thermogravimetric analysis suggested a lower weight loss percentage in case of PANI-Ch-MMT beads (25.7%) followed by PANI-Ch-Ga beads (33.21%), PANI-Ch-MMT microspheres (42.89%) and PANI-Ch-Ga microspheres (51.41%), respectively. As shown in Fig. 1, the beads composed of PANI-Ch-MMT showed a maximum resistance to temperature (up to 600 °C) followed by PANI-Ch-Ga beads (up to 480 °C), PANI-Ch-MMT microspheres (up to 320 °C) and PANI-Ch-Ga microspheres (200 °C). X-ray diffraction (XRD) analysis confirmed the presence of polyaniline nanoparticles on the surface of nanobiocomposites. The maximum average particle/aggregate size was calculated to be 4.18 nm as per Debye-Scherrer equation.

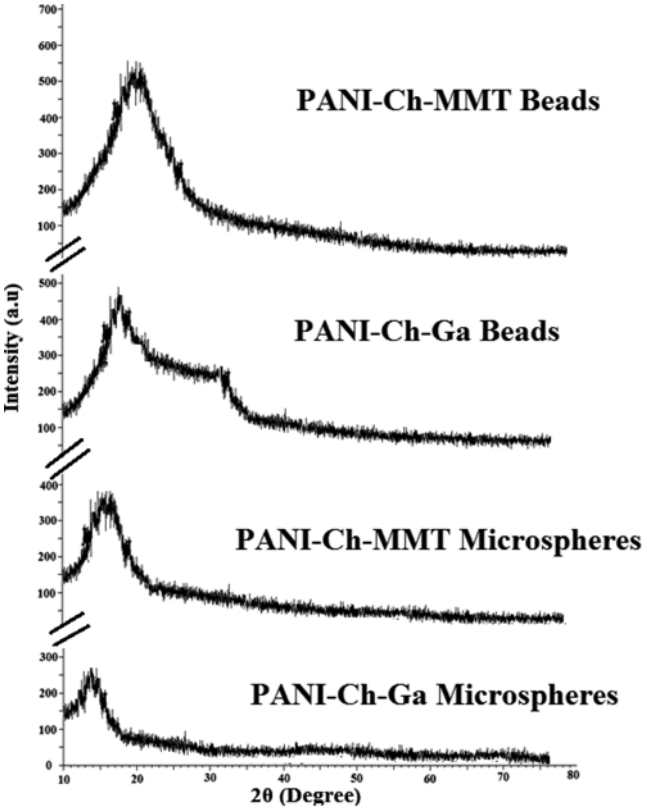

Fig. 2. X-ray diffraction spectra.

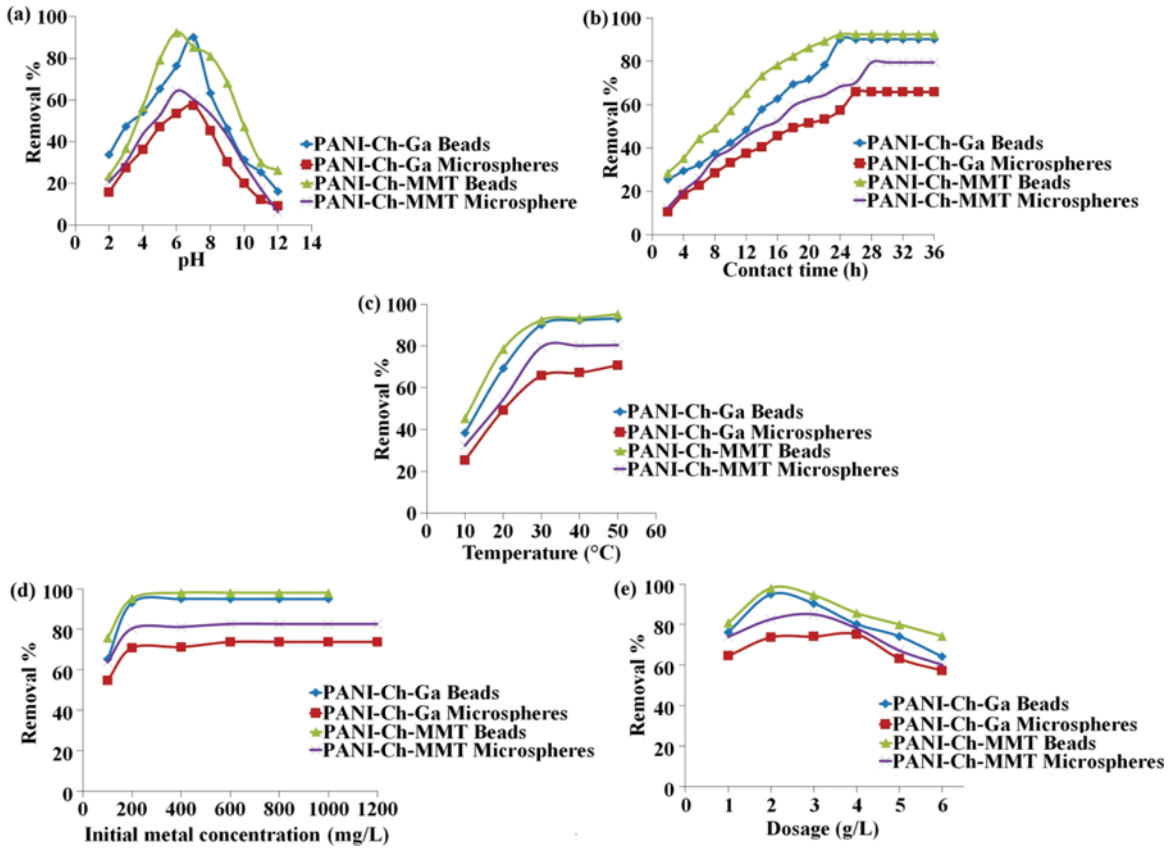

Fig. 3. Effect of parameters (a) pH (Contact time: 24 h; temperature: 30 °C; initial Ni(II) concentration: 200 mg L^{-1}; adsorbent dosage: 2 g L^{-1}), (b) contact time (pH: 6.0 PANI-Ch-MMT beads and microspheres, 7.0 for PANI-Ch-Ga beads and microspheres; temperature: 30 °C; Initial Ni(II) concentration: 200 mg L^{-1}; Adsorbent dosage: 2 g L^{-1}), (c) temperature (pH: 6.0 PANI-Ch-MMT beads and microspheres, 7.0 for PANI-Ch-Ga beads and microspheres; Contact time: 24 h for PANI-Ch-MMT and PANI-Ch-Ga beads, 28 h for PANI-Ch-MMT microspheres, 26 h for PANI-Ch-Ga microspheres; initial Ni(II) concentration: 200 mg L^{-1}; adsorbent dosage: 2 g L^{-1}), (d) initial Ni(II) concentration (pH: 6.0 PANI-Ch-MMT beads and microspheres, 7.0 for PANI-Ch-Ga beads and microspheres; contact time: 24 h for PANI-Ch-MMT and PANI-Ch-Ga beads, 28 h for PANI-Ch-MMT microspheres, 26 h for PANI-Ch-Ga microspheres; temperature: 50 °C; adsorbent dosage: 2 g L^{-1}) and (e) adsorbent dosage (pH: 6.0 PANI-Ch-MMT beads and microspheres, 7.0 for PANI-Ch-Ga beads and microspheres; contact time: 24 h for PANI-Ch-MMT and PANI-Ch-Ga beads, 28 h for PANI-Ch-MMT microspheres, 26 h for PANI-Ch-Ga microspheres; temperature: 50 °C; Initial metal concentration: 400 mg L^{-1} for PANI-Ch-MMT and PANI-Ch-Ga beads, 600 mg L^{-1} for PANI-Ch-MMT and PANI-Ch-Ga microspheres) on Ni(II) removal by nanobiocomposite beads and microspheres.

As shown in Fig. 2, maximum peak intensity of PANI was noted in case of PANI-Ch-MMT beads which exposed the crystallinity of the nanobiocomposite followed by PANI-Ch-GA beads, PANI-Ch-MMT microspheres and PANI-Ch-GA microspheres.

2. Effect of Parameters

The effect of pH on the removal of Ni(II) was examined in the pH range of 2.0 to 12.0 and the data is presented in Fig. 3(a). Results indicated that with an increase in the initial pH of Ni(II) solution, an increase in the net negative charge on the surface of the nanobiocomposite could possibly account for an increase in sorption of Ni(II) ions. An equilibrium was achieved at pH 6.0 in case of PANI-Ch-MMT beads and microspheres and pH 7.0 for PANI-Ch-Ga beads and microspheres. Low Ni(II) removal at pH values lower than the optimum could be due to the competition between positively charged Ni(II) ions and hydrogen ions for the metal binding sites on the adsorbent surface [30].

The removal of Ni(II) by the nanobiocomposites was studied as a function of contact time ranging from 2 to 36 h as shown in Fig. 3(b). The Ni(II) removal efficiency of PANI-Ch-Ga beads, microspheres, PANI-Ch-MMT beads and microspheres reached equilibrium at 24 h, 26 h, 24 h and 28 h, respectively. In the initial stages, the removal of Ni(II) occurred quite rapidly due to the availability of more active sites on the surface of the adsorbent, which resulted in an efficient binding of the metal ions onto the surface functional groups. With successive occupancy of these sites, a consequent decrease in the Ni(II) removal efficiency was noted owing to the repulsion between metal ions present in the solution and metal ions adsorbed on the surface of the nanobiocomposite beads and microspheres [3].

The effect of temperature on the adsorption of Ni(II) was studied in the range of 10-50 °C. Maximum Ni(II) removal was obtained at an optimum temperature of 50 °C in case of all the nanobiocomposites (Fig. 3(c)). The unique relationship between temperature and metal sorption could be attributed to the fact that increase in

temperature results in an enhanced adsorbent swelling, thereby enabling an enhanced diffusion of the Ni(II) metal ions into the adsorbent pores [31].

The effect of initial Ni(II) concentration on the removal efficiency of beads and microspheres was investigated by varying the Ni(II) concentration from 100-1,200 mg L^{-1} (Fig. 3(d)). Maximum sorption was found to occur at an optimum concentration of 400 mg L^{-1} in case of PANI-Ch-MMT beads and PANI-Ch-Ga beads, whereas an upper limit of 600 mg L^{-1} was noted in case of PANI-Ch-MMT microspheres and PANI-Ch-Ga microspheres, respectively. An increase in Ni(II) removal along with the increase in initial metal concentration was due to the availability of sufficient metal ions for the sorption process, which resulted in an increased driving force. However, a further increase in Ni(II) concentration did not show any further enhancement in the Ni(II) uptake due to the saturation of the sites on the nanobiocomposites [32].

The effect of adsorbent dosage on Ni(II) removal was studied by varying the dosage from 1.0 to 6.0 g L^{-1}. As shown in Fig. 3(e), PANI-Ch-MMT beads exhibited the highest Ni(II) removal at a dosage of 2.0 g L^{-1} followed by PANI-Ch-Ga beads (2.0 g L^{-1}), PANI-Ch-MMT microspheres (3.0 g L^{-1}) and PANI-Ch-Ga microspheres (4.0 g L^{-1}). The enhanced Ni(II) removal efficiency along with the increase in adsorbent dosage could be attributed to the increased number of sites and exchangeable ions available for metal adsorption. However, beyond the optimum dosage, a decreasing trend in the removal was noted due to the clumping of the material, thereby decreasing the overall surface area, which could result in the leaching of the pollutant in water. Similar results have been reported in the literature [26].

Based on the above-mentioned results, maximum Ni(II) removal could be achieved by PANI-Ch-MMT beads (98.12%) followed by PANI-Ch-Ga beads (95.02%), PANI-Ch-MMT microspheres (85.12%) and PANI-Ch-Ga microspheres (75.23%) under optimized conditions in batch mode. The results could be attributed to the enhanced exposure of PANI nanoparticles, which rendered the nanobiocomposite a high surface area, thereby leading to an enhanced adsorption of Ni(II) ions from aqueous solution.

3. Equilibrium, Kinetic and Thermodynamic Studies

To examine the relationship between the metal adsorbed on the adsorbent surface and the concentration in the residual solution,

Table 1. Equilibrium isotherm and kinetic model parameters for Ni(II) adsorption on PANI-Ch-Ga and PANI-Ch-MMT nanobiocomposite beads and microspheres

Isotherm models	Parameters	Nanobiocomposites			
		PANI-Ch-Ga		PANI-Ch-MMT	
		Beads	Microspheres	Beads	Microspheres
Langmuir	q_m (mg g^{-1})	120.48	80.64	258.71	151.51
	K_L (L mg^{-1})	0.01	0.01	0.01	$7.3*10^{-3}$
	R^2	0.97	0.97	0.99	0.99
	APE (%)	6.61	15.02	2.22	14.82
Freundlich	n	3.58	1.34	2.81	1.13
	K_F (mg g^{-1})	31.13	1.10	22.13	2.61
	R^2	0.92	0.96	0.90	0.90
	APE (%)	39.53	44.10	48.10	60.88
D-R	q_m (mg g^{-1})	271.40	116.31	232.13	196.33
	E (KJmol^{-1})	0.07	0.02	0.15	0.001
	β (mol^{2}J^{-2})	$1*10^{-4}$	$8*10^{-4}$	$2*10^{-5}$	$5*10^{-4}$
	R^2	0.96	0.98	0.97	0.90
	APE (%)	6.95	10.59	7.10	7.94
Kinetic models					
Pseudo first order	q_e	199.06	124.73	191.86	188.79
	K_1 (min^{-1})	0.07	0.08	0.03	0.07
	R^2	0.96	0.98	0.97	0.97
	APE (%)	1.65	1.66	3.42	2.07
Pseudo second order	q_e	666.66	217.39	500.0	344.82
	K_2 ($gmg^{-1}min^{-1}$)	$2.05*10^{-5}$	$1.59*10^{-4}$	$3.08*10^{-5}$	$7.28*10^{-5}$
	R^2	0.70	0.88	0.82	0.75
	APE (%)	30.92	32.32	18.32	19.86
Intra-particle diffusion	V	35.62	18.63	28.60	27.98
	C	6.88	5.75	46.17	9.74
	R^2	0.98	0.97	0.95	0.98
	APE (%)	3.59	3.67	3.85	3.51

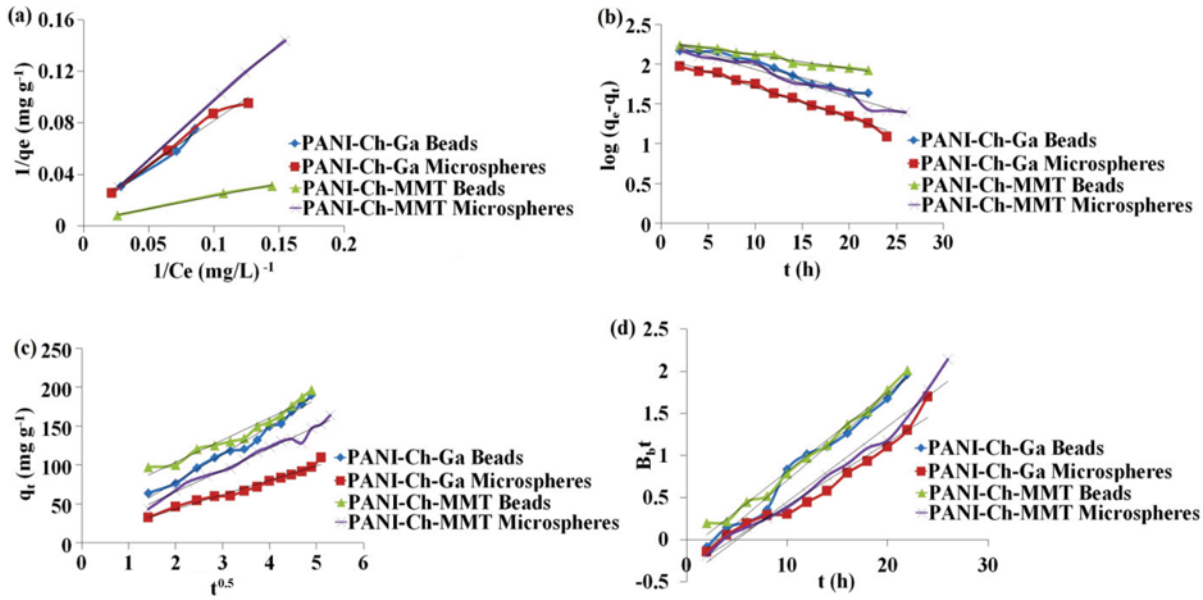

Fig. 4. (a) Langmuir isotherm (b) Pseudo-first-order kinetics (c) Intraparticle diffusion (d) Boyd plot of Ni(II) adsorption onto nanobiocomposite beads and microspheres (Under pre-optimized conditions).

various two parameter isotherms (Langmuir, Freundlich and Dubinin-Radushkevich (D-R)) were employed for fitting the equilibrium data. The isotherm constants, correlation coefficient values (R^2) and average percentage error values (APE%) were calculated and presented in Table 1. Among the isotherm model tested, Langmuir was found to exhibit the best fit for both nanobiocomposite beads and microspheres as shown in Fig. 4(a), thereby suggesting a homogeneous monolayer mode of Ni(II) adsorption owing to their low APE values and high R^2 values. The results of the present study also indicate that the Freundlich model exhibited a poor fit showing low R^2 values and high APE values. The data on mean free energy (E) from D-R isotherm model suggest that a higher amount of energy is required for the removal of Ni(II) from PANI-Ch-MMT beads when compared to other nanobiocomposites thereby confirming a higher affinity between Ni(II) and PANI-Ch-MMT beads.

For the selection of optimum operating conditions in case of full scale batch process, information on kinetics of pollutant uptake is required. To understand the nature of the adsorption process, various kinetic models (pseudo-first-order, pseudo-second-order, intra-particle diffusion and Boyd plot) were evaluated. Various kinetic parameter constants are presented in Table 1. In the present case, the results suggest that pseudo-first-order model exhibited the best fit among all the models in all the cases owing to their high R^2 values and low APE values, thereby indicating physisorption as underlying phenomenon for the adsorption process (Fig. 4(b)). The intraparticle diffusion coefficient for the adsorption of Ni(II) onto PANI-Ch-MMT and PANI-Ch-Ga beads and microspheres was calculated from the slope of the plot between the amount of Ni(II) adsorbed q_t (mg g^{-1}) vs $t^{0.5}$ (min) as shown in Fig. 4(c). High R^2 values and low APE values for intraparticle diffusion model compared to other kinetic models signified the validation of the model (Table 1). The kinetic data were further analyzed using Boyd plot to check whether the sorption proceeds via film diffusion or intraparticle diffusion mechanism. The plot in the present case was found to be linear but did not pass through the origin (Fig. 4(d)), which clearly indicates that both film diffusion and intraparticle diffusion played a role in the adsorption process.

Table 2. Thermodynamic parameters ofNi(II) adsorption on PANI-Ch-Ga and PANI-Ch-MMT nanobiocomposite beads and microspheres

Nanobiocomposites	Temperature (K)	ΔH^o (kJ/mol)	ΔS^o (kJ/mol/K)	ΔG^o (kJ/mol)
PANI-Ch-Ga Beads	283	+31.69	+0.128	−4.53
	293			−5.81
	303			−7.09
	313			−8.37
	323			−9.65
PANI-Ch-Ga Microspheres	283	+37.62	+0.144	−3.13
	293			−4.57
	303			−6.01
	313			−7.45
	323			−8.89
PANI-Ch-MMT Beads	283	+34.21	+0.129	−2.29
	293			−3.58
	303			−4.87
	313			−6.61
	323			−7.45
PANI-Ch-MMT Microspheres	283	+35.13	+0.133	−2.50
	293			−3.83
	303			−5.16
	313			−6.49
	323			−7.82

To describe the thermodynamic behavior of adsorption of Ni(II) onto PANI-Ch-Ga and PANI-Ch-MMT beads and microspheres, thermodynamic parameters (ΔG, ΔH, ΔS) were calculated from standard equations and presented in Table 2. The process was found to be spontaneous with the increase in temperature, which was indicated by negative values of the standard Gibb's free energy (ΔG) and maximum spontaneity was noted at 50 °C in all the cases. The values of ΔH and ΔS were calculated from the slope and intercept of the plot of (q_e/C_e) vs1/T (Fig. 5). The positive values of the standard enthalpy (ΔH) indicated the adsorption as an endothermic process or heat absorbing in nature. The positive values of standard entropy (ΔS) suggested an increase in randomness at the solid/solution interface during the adsorption of Ni(II) on the nanobiocomposites.

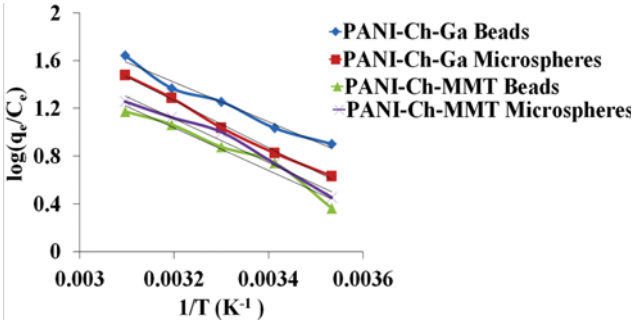

Fig. 5. Thermodynamic studies for adsorption of Ni(II) onto nanobiocomposite beads and microspheres (Experiments were carried out under conditions optimized in batch studies).

4. Instrumental Analysis

To identify the possible interaction between gum (Ga) based and clay (MMT) based nanobiocomposite beads and Ni(II), the surface functional groups of the adsorbent were characterized by FT-IR before and after adsorption (Fig. 6(a)-(d)). A high involvement of secondary amines (NH stretch (3,301.24 cm^{-1}), (NH bend (1,548.13 cm^{-1}) was noted in case of PANI-Ch-MMT beads (Fig. 6(d)) as compared to that of PANI-Ch-Ga beads (Fig. 6(c)) after Ni(II) adsorption. Additional involvement of alkyls (2,945.30 cm^{-1}), anhydrides (1,737.86 cm^{-1}), alcohols (1,365.60 cm^{-1}, 1,352.10 cm^{-1} and 833.25 cm^{-1}), esters (1,215.15 cm^{-1} and 1,020.89 cm^{-1}) and aldehydes (648.08 cm^{-1}) was noted in case of PANI-Ch-MMT beads after Ni(II) adsorption. In case of PANI-Ch-Ga beads, the involvement of anhydrides, alcohols and aldehydes was not found to play an important role in the adsorption process. The involvement of greater number of functional groups and the changes in the overall transmittance was found to be higher in case of PANI-Ch-MMT beads as compared to that of PANI-Ch-Ga beads, which validated PANI-Ch-MMT beads as potential adsorbent for the remediation of Ni(II) ions from aqueous solution.

The analysis of PANI-Ch-MMT and PANI-Ch-Ga beads using scanning electron microscopy (SEM) was conducted to get further insight into the surface morphology before and after Ni(II) adsorption (Fig. 7(a)-(d)). The SEM image of the nanobiocomposite beads before Ni(II) adsorption (Fig. 7(a)-(b)) revealed that the

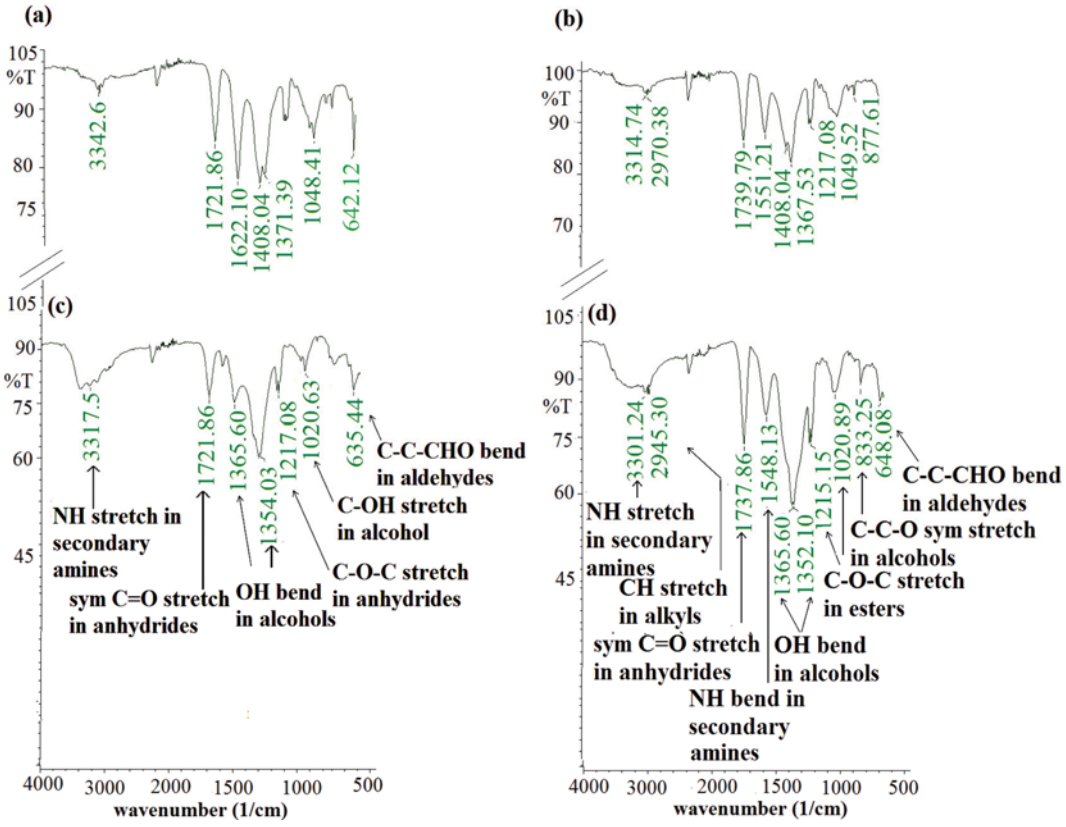

Fig. 6. FT-IR spectra of PANI-Ch-Ga beads and PANI-Ch-MMT beads before (a) and (b) after (c) and (d) Ni(II) adsorption.

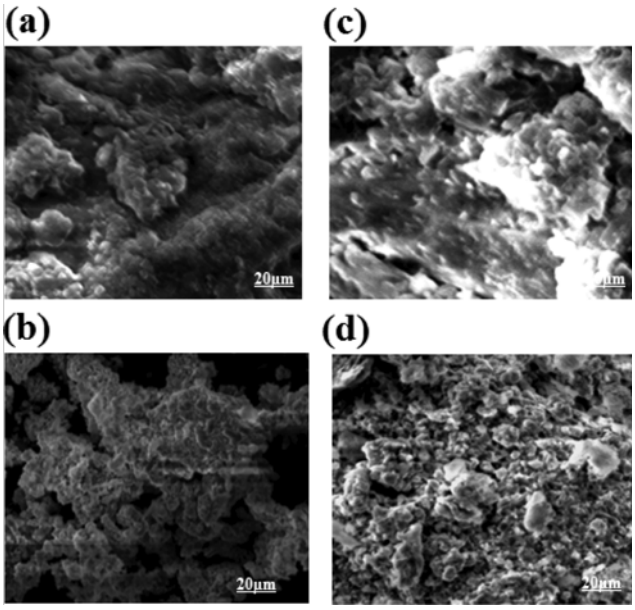

Fig. 7. SEM analysis of PANI-Ch-Ga beads and PANI-Ch-MMT beads before (a) and (b) after (c) and (d) Ni(II) adsorption.

particles were irregular in shape and mostly present in aggregation. Moreover, the surface was found to be rough due to polymerization of aniline providing a good possibility for the metal ions to be trapped and adsorbed and was found to be in accordance with the literature [33]. After Ni(II) adsorption (Fig. 7(c)-(d)), a homogeneous surface coverage was noted, which validated the Langmuir isotherm. Moreover, in case of PANI-Ch-MMT beads (Fig. 7(d)), a more electron dense part (bright region) appeared, which was due to nickel adsorption compared to PANI-Ch-Ga beads (Fig. 7(c)). Similar result was reported in case of Ni(II) removal using sericite beads [34].

However, to confirm whether the electron dense part on the surface of the nanobiocomposite was composed of nickel ions, the elemental analysis of PANI-Ch-MMT and PANI-Ch-Ga beads before and after Ni(II) adsorption was carried out using energy dispersive X-ray (EDX) analysis (Fig. 8(a)-(d)).

The EDX spectrum of PANI-Ch-Ga beads before Ni(II) adsorption indicated the presence of C,O and N as natural species on the surface of the nanobiocomposite (Fig. 8(a)), whereas the peaks of Na, Si and Al confirmed the presence of clay on PANI-Ch-MMT beads (Fig. 8(b)). After Ni(II) adsorption an intense Ni(II) peak was observed in case of PANI-Ch-MMT beads (Fig. 8(d)) as compared to PANI-Ch-Ga beads (Fig. 8(c)). In case of PANI-Ch-MMT beads, a certain decrease in the peaks of Na, Al and Si was noted after Ni(II) adsorption, which confirmed their involvement in the adsorption process (Fig. 8(d)). For both the nanobiocomposites, a significant decrease in the C and O peaks was noted, which validated their involvement in the adsorption process. Moreover, a higher decrease in C peak in case of PANI-Ch-MMT beads confirmed its higher uptake potential compared to PANI-Ch-Ga beads.

5. Effect of Co-ions

Among the co-ions (Zn(II) and Cu(II)) tested, Zn(II) was found to exhibit a predominant effect on Ni(II) adsorption followed by Cu(II) owing to their difference in ionic radii. To study the metal-metal interaction with the adsorbent, an interaction factor (η) was specifically noted for both binary and ternary systems.

The extended Langmuir and SRS equation parameters for binary and ternary systems were calculated and presented in Table 3. The interaction factor (η_2) based on the extended Langmuir equation was found to be the highest for both PANI-Ch-Ga beads (2.32) and PANI-Ch-MMT beads (1.87), which signified that zinc had the most predominant effect on Ni(II) adsorption. The interaction factors were found to be higher for the ternary system when compared to binary system in the case of both PANI-Ch-Ga beads and PANI-Ch-MMT beads. Moreover, lower interaction factors

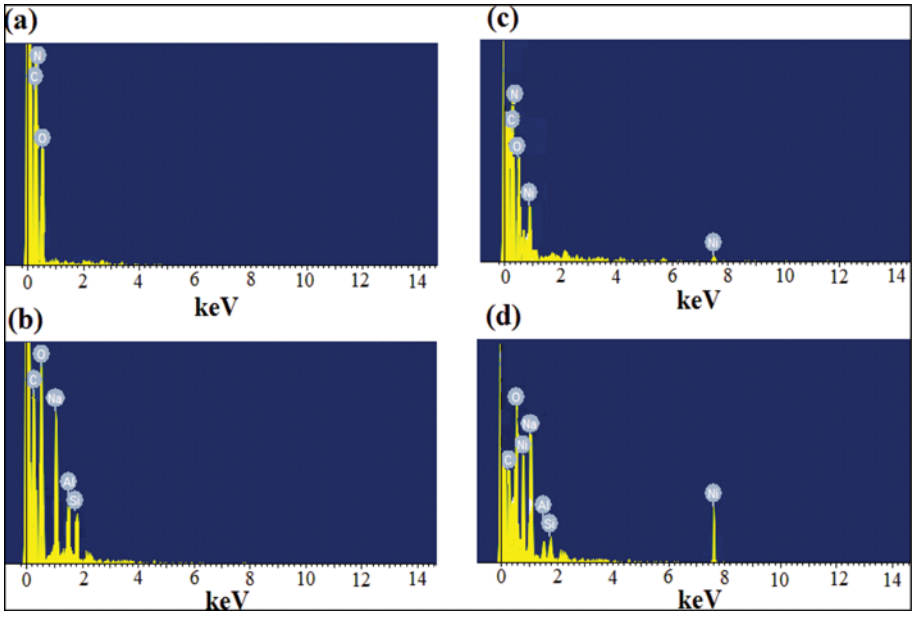

Fig. 8. EDX spectra of PANI-Ch-Ga beads and PANI-Ch-MMT beads before (a) and (b) after (c) and (d) Ni(II) adsorption.

Table 3. Extended Langmuir and SRS equation parameters for binary and ternary systems

Extended Langmuir				SRS			
	Ni-Zn		Ni-Zn-Cu		Ni-Zn		Ni-Zn-Cu
PANI-Ch-Ga Beads							
η_1	0.18	η_1	0.31	K_{Fi}	31.13	K_{Fi}	31.13
η_2	2.32	η_2	2.67	n_i	3.07	n_i	3.07
b_1	0.06	η_3	1.02	θ_{ij}	1.2	θ_{ij}	2.7
b_2	0.43	b_1	0.06	APE (%)	8.02	APE (%)	12.37
APE (%)	58.52	b_2	0.43	R^2	1.0	R^2	1.0
R^2	1.0	b_3	0.25				
		APE (%)	25.30				
		R^2	1.0				
PANI-Ch-MMT Beads							
η_1	0.12	η_1	0.22	K_{Fi}	22.13	K_{Fi}	22.13
η_2	1.87	η_2	2.04	n_i	2.12	n_i	2.12
b_1	0.04	η_3	0.75	θ_{ij}	2.7	θ_{ij}	4.3
b_2	0.32	b_1	0.04	APE (%)	12.40	APE (%)	23.84
APE (%)	50.66	b_2	0.32	R^2	1.0	R^2	1.0
R^2	1.0	b_3	0.36				
		APE (%)	47.26				
		R^2	1.0				

were noted in case of PANI-Ch-MMT beads, thereby suggesting a lower level of competition between Ni(II) and co-ions when compared to that of PANI-Ch-Ga beads (Table 3). The selectivity factor was calculated and found to be 1.12 (Ni-Zn) and 1.06 (Ni-Cu) in case of PANI-Ch-Ga beads, whereas in case of PANI-Ch-MMT beads, the selectivity factor was 1.36 (Ni-Zn) and 1.13 (Ni-Cu). In all the cases, the selectivity factor was more than 1, which signified that the preference of nickel(II) was highest among other co-ions. Moreover, a maximum selectivity factor was noted for PANI-Ch-MMT beads, thereby denoting a preferential adsorption of Ni(II) ions as compared to PANI-Ch-Ga beads.

To improve the fitness, the SRS equation was used to describe the binary and ternary data. The model consisted of a competitive coefficient (θ), which presumes an exponential distribution of adsorption energies available for each metal ion. As expected the competition coefficient was lower in case of binary system as compared to ternary system, suggesting a lower level of competition for Ni(II) adsorption in case of binary system (Table 3). The competitive coefficient was noted to be higher for PANI-Ch-MMT beads when compared to PANI-Ch-Ga beads, which validated the adsorption potential of the former over the later. The results also suggested a better distribution of adsorption energies for the metal ions in case of PANI-Ch-MMT beads compared to PANI-Ch-Ga beads (Fig. 9).

Based on the correlation coefficient values and error values, it could be inferred that the SRS model exhibited a better fit for both PANI-Ch-MMT and PANI-Ch-Ga beads when compared to that of extended Langmuir model.

6. *Ex-situ* Studies

6-1. Effect of Column Parameters

Column studies were conducted in glass column packed with PANI-Ch-MMT beads. The removal of Ni(II) was studied as a

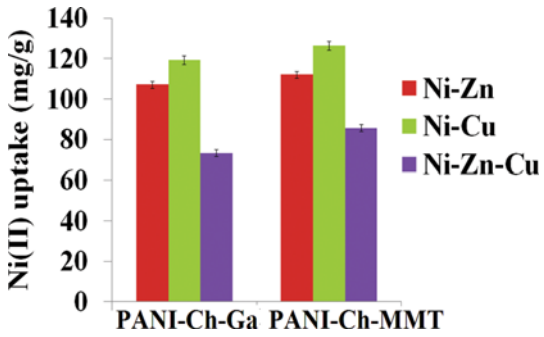

Fig. 9. Effect of co-ions on adsorption of Ni(II) on PANI-Ch-Ga beads and PANI-Ch-MMT beads.

function of parameters: bed height (4 cm, 8 cm and 12 cm), flow rate (1 mL min^{-1}, 3 mL min^{-1} and 5 mL min^{-1}) and effluent dilutions (0%, 25% and 50%) and the breakthrough curves are presented in Fig. 10(a)-(c). The efficiencies were estimated in terms breakthrough time (t_b), exhaustion time (t_e), total amount of pollutant sent to the column (M_{total}), amount of pollutant adsorbed (M_{ad}) and removal (%). Table 4 shows that the breakthrough time (t_b) and exhaustion time (t_e) increased with the increase in bed height. High percentage of Ni(II) removal was noted at maximum bed height 12 cm maintaining flow rate of 1 ml/min and 0% dilution. This could be attributed to the fact that a taller bed will provide more adsorbent sites to which Ni(II) ions could bind [35]. The effect of flow rate on the removal of Ni(II) from the wastewater was studied at maximum bed height (12 cm) and 0% dilution. Contrary to the result obtained in case of bed height, a decrease in the breakthrough time and exhaustion time was noted with the increase in flow rate. Maximum removal was obtained at the minimum flow rate (1 mL min^{-1}), beyond which a decrease was noted due to insuffi-

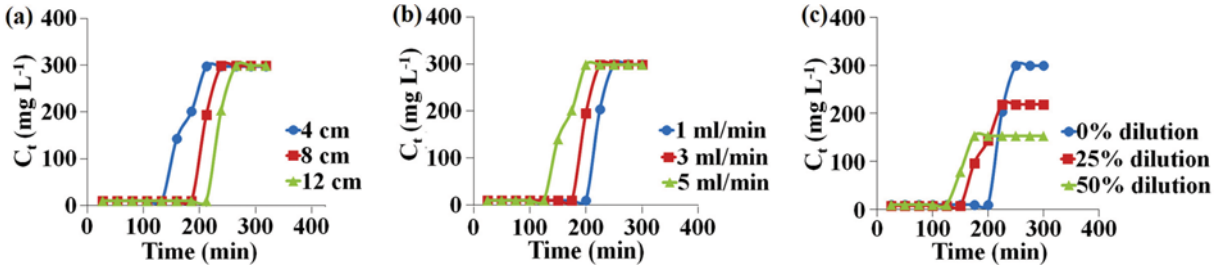

Fig. 10. Breakthrough curves for adsorption of Ni(II) onto PANI-Ch-MMT beads (a) at different bed heights (flow rate - 1 mL min^{-1}, dilution-0%) (b) at different flow rates (bed height - 12 cm, dilution-0%) (c) at different dilutions (bed height 12 cm, flow rate 1 mL min^{-1}).

Table 4. Column parameters obtained at different bed heights, flow rates and dilutions for nickel(II) adsorption

	4 cm	8 cm	12 cm
	Bed height (flow rate- 1 ml/min; dilution- 0%)		
t_b (min)	125	175	200
t_e (min)	200	225	250
M_{total}	60.00	67.50	75.00
M_{ad}	42.67	53.42	60.41
Efficiency (%)	71.12	79.14	80.55
	1 mL min^{-1}	3 mL min^{-1}	5 mL min^{-1}
	Flow rate (bed height- 12 cm; dilution- 0%)		
t_b (min)	200	175	125
t_e (min)	250	225	200
M_{total}	75.00	67.50	60.00
M_{ad}	60.41	53.38	42.72
Efficiency (%)	80.55	79.08	71.20
	0%	25%	50%
	Dilution (bed height- 12 cm; flow rate- 1ml/min)		
t_b (min)	200	150	125
t_e (min)	250	225	175
M_{total}	75.00	49.50	27.12
M_{ad}	60.41	36.80	20.05
Efficiency (%)	80.55	74.36	73.92

cient residence time of the metal ions in the column [36]. Various dilutions were performed at maximum bed height (12 cm) and minimum flow rate (1 mL min^{-1}) in order to study the effect of dilutions on Ni(II) adsorption. The breakthrough time (t_b) and adsorbed metal (M_{ad}) were found to be maximum in case of 0% dilution and decreased with increase in dilution. Maximum Ni(II) removal (80.55%) was noted in undiluted wastewater (0% dilution), which can be attributed to the fact that the availability of metal ions is much higher in this case, which leads to higher uptake of metal ions when compared to that of diluted wastewater (25% and 50% dilution).

6-2. Column Data Modelling

Various mathematical models have been developed for lab scale column data analysis. One of the most applied models for adsorption of heavy metals in column mode is the bed depth service time (BDST) model, which states the relation between the bed height (cm) and service time (min). Fig. 11(a) shows the plot of service time vs bed height at various dilutions maintaining the flow rate of 1 mL min^{-1}. The BDST model parameters are shown in Table 5 and the equation of linear relationship was obtained with R^2 value of 0.99, which indicated the validity of BDST model for the present column study. As shown in Table 5, the column sorption capacity (N_0) was found to decrease with an increase in dilution owing to the reduction in the concentration of metal sent through the column. The rate constant (K_a) values showed a decrease in trend (the least being in the case of 50% dilution), which indicated that a progressively longer bed was required to avoid breakthrough [37].

The Thomas model was also used in the present study to evaluate column breakthrough data. The model parameters were calculated based on the plot of $\ln((C_0/C_t)-1)$ vs volume of effluent treated (V_{eff}) (Fig. 11(b)) and presented in Table 5. Based on the correlation coefficient value (R^2: 0.99), the model exhibited a good fit. The rate constant (K_{TH}), the parameter which characterizes the rate of sol-

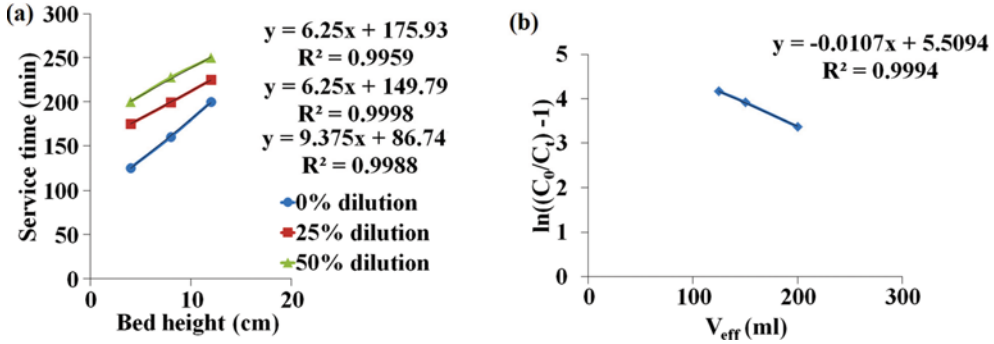

Fig. 11. (a) BDST model (b) Thomas model.

Table 5. Bed depth service time model and Thomas model parameters for adsorption of Ni(II) on PANI-Ch-MMT beads at different effluent dilutions

	Effluent dilutions		
	0%	25%	50%
BDST parameters			
Slope	6.250	6.250	9.375
Intercept	175.93	149.79	86.74
N_o (mg/L)	396.56	193.87	136.59
K_a (L/mg/min)	$1.29*10^{-4}$	$9.92*10^{-5}$	$9.79*10^{-5}$
R^2	0.995	0.999	0.998
Thomas parameters			
V_{eff}	200	150	125
C_o	300	220	155
K_{TH} (min^{-1})	$3.56*10^{-5}$	$4.86*10^{-5}$	$6.90*10^{-5}$
Q_o (mg/g)	309.51	226.72	159.69

ute transfer from solid to liquid phase was found to increase with an increase in dilution, which signified a higher sorption rate due to availability of more surface functional groups at a low metal concentration [37].

An experiment was conducted with mining wastewater using a packed bed column under optimum conditions (bed height: 12 cm, flow rate: 1 mL min^{-1} and dilution: 0%). Analysis of waster showed that apart from removal of Ni(II) ions, a decrease in the overall COD, BOD, chlorides, sulfates, nitrates and heavy metals was also noted as shown in Table 6, which justified the adsorption potential of the PANI-Ch-MMT beads.

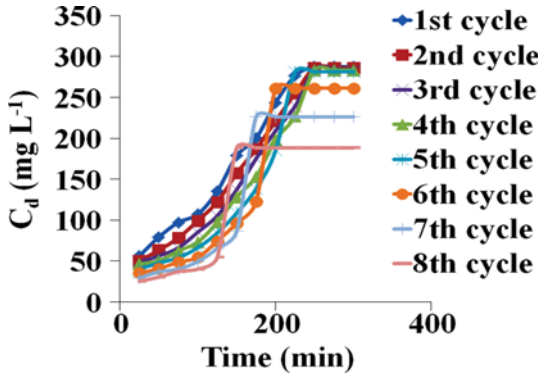

Fig. 12. Reuse of PANI-Ch-MMT beads during eight regeneration cycle (bed height: 12 cm; flow rate: 1 mL min^{-1}; dilution: 0%).

7. Regeneration Studies

The reusable nature of the adsorbent was tested for eight cycles by alternating between adsorption and desorption using the column mode of operation (Fig. 12). The breakthrough time (t_b), exhaustion time (t_e), total metal ions sent to the column (M_{total}), total quantity of metal mass adsorbed in the column (M_{ad}), total quantity of metal mass desorbed from the column (M_d), removal percentage and desorption percentage for eight cycles were calcu-

Table 6. Analysis of mining wastewater

Parameters	Before treatment with PANI-Ch-MMT beads	After treatment with PANI-Ch-MMT beads
pH	6.0	6.5
Colour	Grey	Colourless
Total dissolved solids (mg/L)	765.28±0.06	48.27±0.09
Biochemical oxygen demand (mg/L)	1102.3±0.01	210.3±0.21
Chemical oxygen demand (mg/L)	923.1±0.05	127.4±0.14
Chlorides (Cl^{-1}) (mg/L)	223.4±0.21	58.2±0.25
Sulfate (SO_4^{2-}) (mg/L)	142.5±0.15	42.2±0.16
Nitrates (NO_3^-) (mg/L)	321.5±0.06	107.3±0.31
Nickel(II) (mg/L)	300.0±0.24	3.4±0.07
Copper(II) (mg/L)	142.4±0.15	1.2±0.12
Zinc(II) (mg/L)	110.2±0.26	1.5±0.28

Table 7. Adsorption and desorption process parameters for different sorption-desorption cycles

Parameters	No. of cycles							
	1	2	3	4	5	6	7	8
t_b (min)	200	200	200	200	175	150	125	100
t_e (min)	250	250	250	250	225	200	175	150
M_{total} (mg)	75.0	75.0	75.0	75.0	67.5	60.0	52.5	45.0
M_{ad} (mg)	60.4	59.7	59.0	58.7	51.1	39.5	24.9	16.7
M_d (mg)	37.9	34.4	31.6	29.4	21.6	15.0	10.5	7.0
Removal (%)	80.5	79.6	78.7	78.3	75.8	65.9	47.6	37.1
Desorption (%)	50.5	45.9	42.1	39.2	32.0	25.1	20.0	15.6

Table 8. Reported works on Ni(II) uptake using different adsorbents

Adsorbents	Ni(II) uptake (mg/g)	References
Tea factory waste	15.26	[31]
Coir pith	15.95	[30]
Multiwalled Carbon nanotubes	49.26	[4]
Punica granatum peel waste	52.00	[39]
Chemically activated carbon	18.00	[38]
γ-Alumina nanoparticles	49.70	[6]
PANI-Ch-Ga beads	190.00	[Present study]
PANI-Ch-Ga microspheres	109.50	[Present study]
PANI-Ch-MMT beads	196.54	[Present study]
PANI-Ch-MMT microspheres	164.00	[Present study]

lated and are summarized in Table 7. The maximum removal was noted as 80.55% in the first cycle after which a decreasing trend was noted that could be attributed to the damages on the surface of the nanobiocomposite due to continuous contact with desorbing agent (0.1 M HNO_3). The decrease in nickel removal percentage was found to be insignificant till the fifth cycle, after which a drastic decrease was noted. This suggested that PANI-Ch-MMT beads could be reused up to five cycles. Table 8 represents the reported work on Ni(II) adsorption using various adsorbents.

CONCLUSION

We report the application of gum based and clay based polyaniline/chitosan nanobiocomposite beads and microspheres for the removal of Ni(II) from aqueous environments. Maximum Ni(II) removal (98.12%) was shown by PANI-Ch-MMT beads under optimized conditions (pH: 6.0, time: 24 h, temperature: 50 °C, initial Ni(II) concentration: 400 mg L^{-1}, adsorbent dosage: 2 g L^{-1}). Equilibrium and kinetic studies were performed to study the mode and rate of adsorption. The surface homogeneity of the PANI-Ch-MMT beads was confirmed by Langmuir isotherm model. The adsorption kinetic data was well described by pseudo-first-order model, which suggested a physical mode of adsorption via both intra-particle and film diffusion. Thermodynamic studies defined the adsorption process as endothermic. *Ex-situ* studies were performed using a packed-bed column for removal of Ni(II) ions from mining wastewater at varying bed heights (4 cm, 8 cm and 12 cm), flow rates (1 mL min^{-1}, 3 mL min^{-1} and 5 mL min^{-1}) and dilutions (0%, 25% and 50%). Maximum Ni(II) removal from wastewater (up to 80.55%) was noted under optimum conditions (bed height: 12 cm, flow rate: 1 mL min^{-1} and dilution 0%). The regeneration studies suggest that PANI-Ch-MMT beads could be effectively reused up to five cycles. Based on the results of the present study, it can be suggested that PANI-Ch-MMT beads can serve as an excellent and reliable adsorbent for the remediation of Ni(II) ions from wastewater.

ACKNOWLEDGEMENT

The authors are grateful to VIT University for providing the necessary laboratory facilities. We take this opportunity to thank SEM lab and TBI, VIT University who helped us for the instrumental analysis.

REFERENCES

1. N. Unlua and M. Ersoz, *J. Hazard. Mater.*, **136**, 272 (2006).
2. I. S. Kwak, S. W. Won, S. B. Choi, J. Mao, S. Kim, B. W. Chung and Y. S. Yun, *Korean J. Chem. Eng.*, **28**, 927 (2011).
3. L. He, B. B. Wang, D. D. Liu, K. S. Qian and H. B. Xu, *Korean J. Chem. Eng.*, **31**, 343 (2014).
4. M. I. Kandah and J. L. Meunier, *J. Hazard. Mater.*, **146**, 283 (2007).
5. S. P. Parker, *Encyclopedia of Environmental Science*, 2nd Ed. McGraw Hill, New York (1980).
6. M. Fouladgar, M. Beheshti and H. Sabzyan, *J. Mol. Liq.*, **211**, 1060 (2015).
7. M. Y. Can, Y. Kaya and O. F. Algur, *Bioresour. Technol.*, **97**, 1761 (2006).
8. K. Kalantari, M. B. Ahmad, H. R. F. Masoumi, K. Shameli, M. Basri and R. Khandanlou, *J. Taiwan Inst. Chem. Eng.*, **49**, 192 (2015).
9. R. Celis, M. A. Adelino, M. C. Hermosín and J. Cornejo, *J. Hazard. Mater.*, **209**, 67 (2012).
10. E. S. A. Halim and S. S. Al. Deyab, *Carbohydr. Polym.*, **84**, 454 (2011).
11. W. Nitayaphat and T. Jintakosol, *J. Clean Prod.*, **87**, 850 (2015).
12. S. S. Banerjee and D. H. Chen, *J. Hazard. Mater.*, **147**, 792 (2007).
13. P. Wu, Q. Zhang, Y. Dai, N. Zhu, Z. Dang, P. Li, J. Wu and X. Wang, *Geoderma*, **164**, 215 (2011).
14. A. R. Nesic, S. J. Velickovic and D. G. Antonovic, *J. Hazard. Mater.*, **209**, 256 (2012).
15. J. Stejskal, I. Sapurina and M. Trchová, *Prog. Polym. Sci.*, **35**, 1420 (2010).
16. V. Janaki, B. T. Oh, K. Shanthi, K. J. Lee, A. K. Ramasamy and S. K. Kannan, *Synth. Met.*, **162**, 974 (2012).
17. S. M. Ahmed, F. I. El-Dib, N. S. El-Gendy, W. M. Sayed and M. El-Khodary, *Arab. J. Chem.* (2012), DOI:10.1016/j.arabjc.2012.04.049.
18. D. Das, L. R. Varghese and N. Das, *Desalination*, **360**, 35 (2015).
19. L. Zhou, Y. Wang, Z. Liu and Q. Huang, *J. Hazard. Mater.*, **161**, 995 (2009).
20. Z. E. Khalid, G. O. El. Sayed and R. S. Darweesh, *Inter. J. Min. Proc.*, **120**, 26 (2013).
21. I. Langmuir, *J. Am. Chem. Soc.*, **38**, 2221 (1916).
22. H. M. F. Freundlich, *J. Phys. Chem. B.*, **57**, 385 (1906).
23. M. M. Dubinin, *Chem. Rev.*, **60**, 235 (1960).
24. Y. S. Ho, *Scientometrics.*, **59**, 171 (2004).
25. Y. S. Ho, *Water Res.*, **40**, 119 (2006).
26. D. Das, G. Basak, V. Lakshmi and N. Das, *Biochem. Eng. J.*, **64**, 30 (2012).
27. S. A. Khan, R. Rehman and M. A. Khan, *Waste Manage.*, **15**, 271 (1995).
28. K. Vijayaraghavan and R. Balasubramanian, *Chem. Eng. J.*, **163**, 337 (2010).
29. V. Vinodhini and N. Das, *Desalination*, **264**, 9 (2010).
30. H. Parab, S. Joshi, N. Shenoy, A. Lali, U. S. Sarma and M. Sudersanan, *Process Biochem.*, **41**, 609 (2006).
31. E. Malkoc and Y. Nuhoglu, *J. Hazard. Mater.*, **127**, 120 (2005).
32. E. Malkoc, *J. Hazard. Mater.*, **137**, 899 (2006).

33. V. Janaki, K. Vijayaraghavan, B. T. Oh, K. J. Lee, K. Muthuchelian, A. K. Ramasamy and S. K. Kannan, *Carbohydr. Polym.*, **90**, 1437 (2012).
34. C. Jeon and J. H. Cha, *J. Ind. Eng. Chem.*, **24**, 107 (2014).
35. D. Charumathi and N. Das, *Desalination*, **285**, 22 (2012).
36. J. B. Zambrano, A. Szygula, M. Ruiz, A. M. Sastre and E. Guibal, *J. Environ. Manage.*, **91**, 2669 (2010).
37. D. Das, J. S. Varshini and N. Das, *Miner. Eng.*, **69**, 40 (2014).
38. H. Runtti, S. Tuomikoskia, T. Kangas, U. Lassi, T. Kuokkanen and J. Rämö, *J. Water Process. Eng.*, **4**, 12 (2014).
39. A. Bhatnagar and A. K. Minocha, *Colloids Surf., B.*, **76**, 544 (2010).